University of Trento
Department of Industrial Engineering

UNIVERSITY OF TRENTO

Precision engineering

Project Work

High Precision Linear Displacement Measurement System

Professor:
Prof. Paolo Bosetti

Group:
I

Student:
Lorenzo Colturato, 233301

Academic Year 2021-2022

Abstract

This report is about the design of a high precision linear displacement measurement system for touch probe applications. Chapter 1 briefly explains what the project is about and the phases through which the realization of the project was possible. Chapter 2 reports the House of Quality which has been developed to gather all the necessary information to carry on the design phase. Chapter 3 is about the presentation in details of the capacitor transducer on which the designed system is based and on which i have personally worked. Finally, Chapter 4 reports the conclusions.

Table of Contents

List of Figures

List of Tables

Chapter 1

Introduction

The aim of the project was to design a high precision linear displacement measurement system for touch probe applications. To do so, the first thing to do is to collect all the information necessary for the design in the House of Quality, which gives the description of the project. After the completion of the House of Quality, the next step is to generate the concepts that allow to give life to the functions that the system to be designed must perform. After the evaluation of the generated concepts through studies and analyses, only one concept must be chosen, which is carried forward to realize the measurement system.

Chapter 2

House of Quality (QFD)

The initial phase of the project concerns the drafting of the House of Quality where all the information that are relevant to the next phases are collected and stated. The House of Quality that was developed for this project is shown in Figure 2.1, containing the customers, the customers requirements, the engineering specifications with the target values and the competitors.

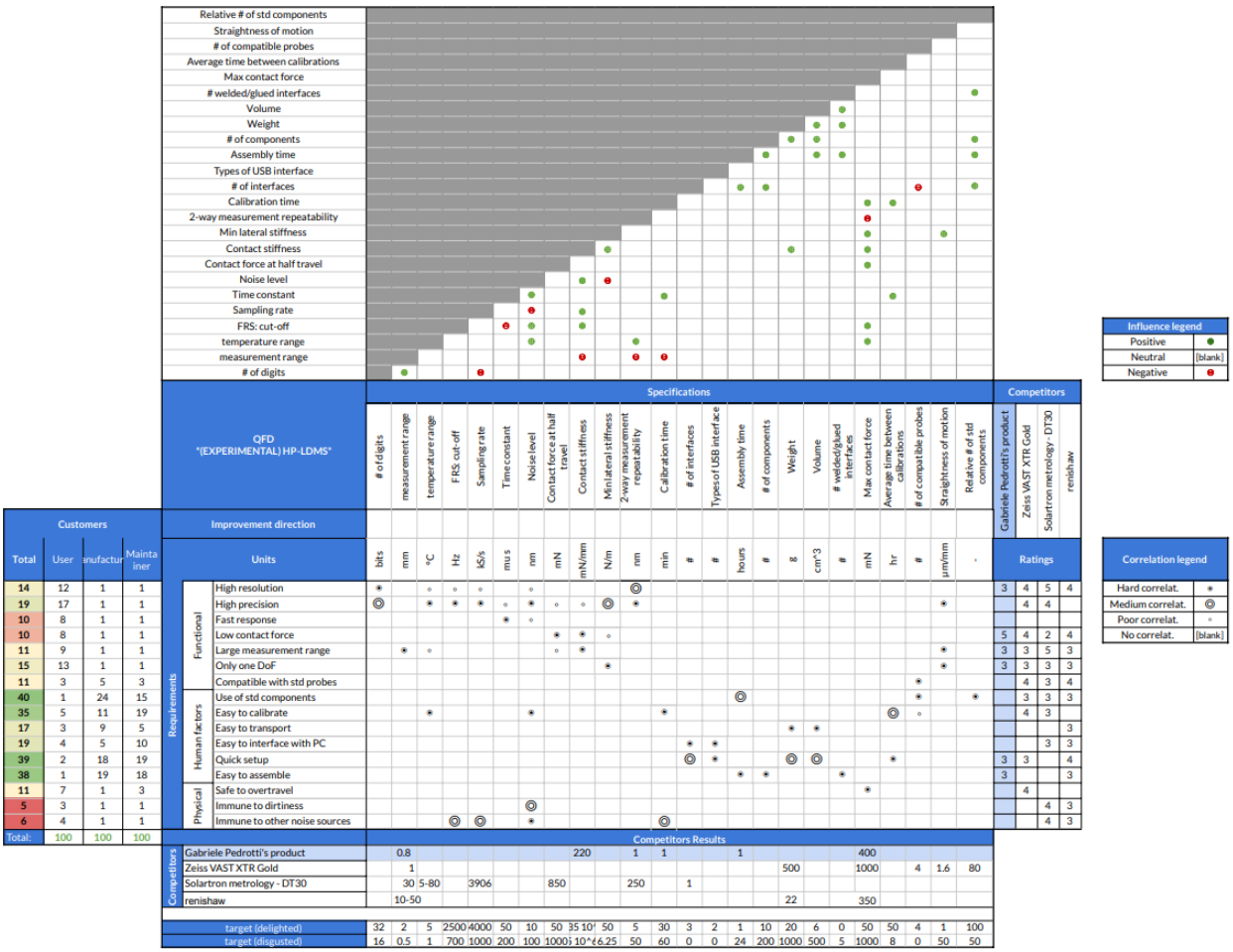

Figure 2.1: House of Quality

Chapter 3

Developed concept

3.1 Introduction

After the QFD was developed, the next step has been the definition of the atomic functions that the system have to perform, i.e the functional decomposition, and the search for the possible implementations to make in practice all the functions, i.e the morphology combination. Three different concepts have been considered and after an analysis on their performances, with the help of a decision matrix based on belief maps, it was decided to design a measurement system based on a capacitor transducer to convert the displacement into a signal of time, with the use of a double compound rectilinear spring to provide the linear motion to the probe tip, allowing so the one degree of freedom of movement.
The project team was mainly divided in two subgroups: one dedicated to the development of the capacitor transducer and the other on the analysis and the sizing of the double compound rectilinear spring. I was part of the group focused on the design of the transducer, which will then be presented in detail on the following pages.

3.2 Capacitor transducer

3.2.1 Principle of operation

Figure 3.1 presents a schematic of the electronic components of the logic circuit that controls the operations of the transducer, which has been developed using *LTspice*.

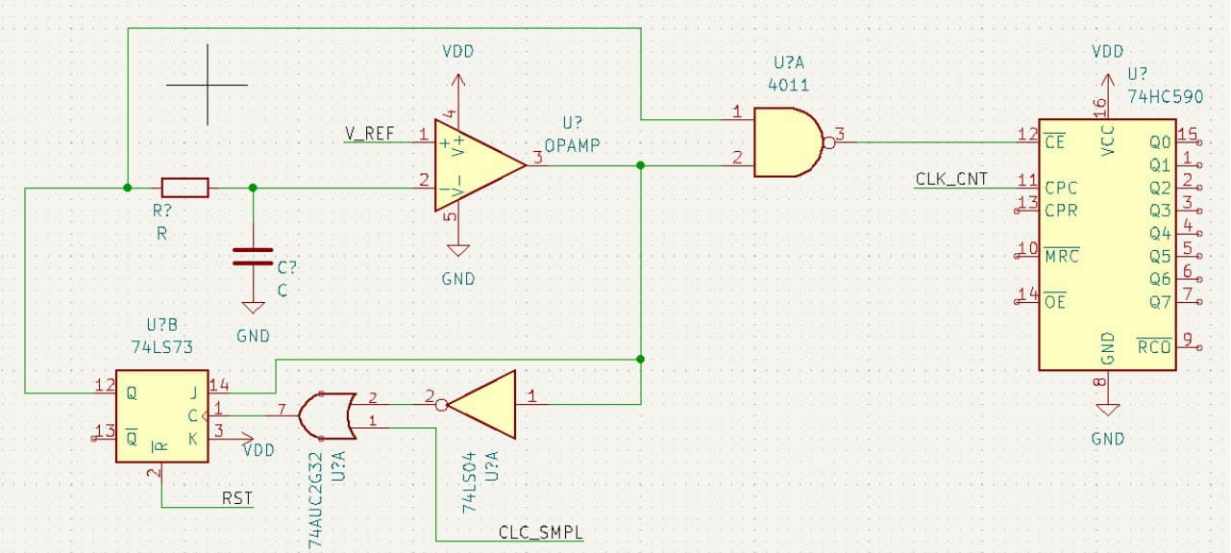

Figure 3.1: Schematic of the electronic components

The fundumental part of the transducer is the RC circuit, consisting of a resistor and a parallel fixed plates capacitor with a dielectric material which instead is movable and, based on the displacement of the probe tip that interacts with the object of measure, moves within the space between the plates, changing the overall capacitance of the capacitor. The dielectric material can be considered infact as an additional capacitance that adds up to the capacitance of the capacitor, hence it is a parallel configuration.
Figure 3.2a shows a 3D visualization of the capacitor and its dimensions: b1 and b2 are the dimensions of the plates, while h is the distance between the plates. In Figure 3.2b is represented a plane view of the capacitor and the dielectric that can move within it, where x is the space occupied by the dielectric inside the capacitor.

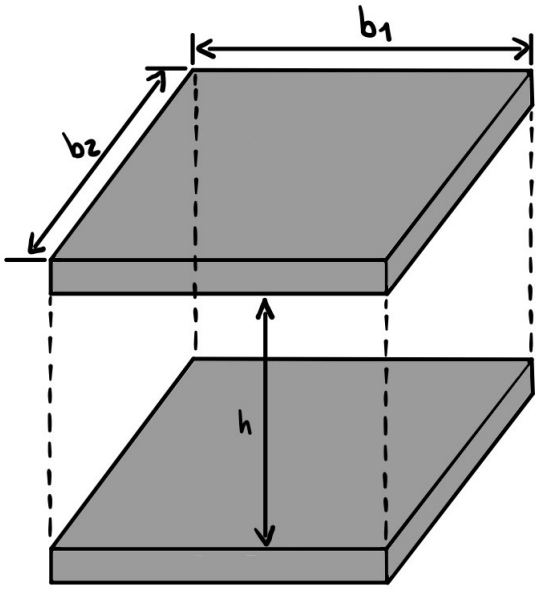

(a) Parallel plate capacitor - 3D view

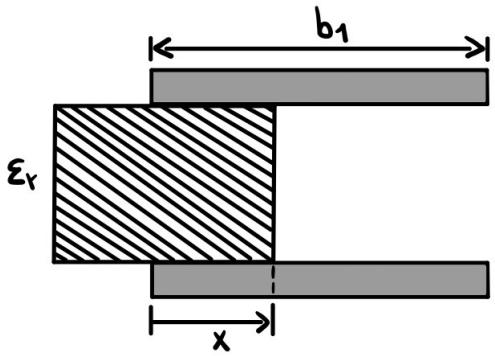

(b) Parallel plate capacitor - 2D view with the insertion of the dielectric

Figure 3.2: Capacitor

The dimension b1 represents the maximum value of the displacement of the dielectric inside the capacitor, therefore the displacement x is limited to assume values in the range $0 \leq x \leq b1$. When the displacement x is larger than zero, the presence of the dielectric material inside the capacitor affect the overall capacitance (C_{eq}), which is therefore a function of x.

$$\text{Capacitance of the dielectric:} \qquad C_1 = \frac{\epsilon_0 \epsilon_r x b_2}{h} \tag{3.1}$$

$$\text{Capacitance of the capacitor:} \qquad C_2 = \frac{\epsilon_0 (b_1 - x) b_2}{h} \tag{3.2}$$

$$\text{Overall capacitance:} \qquad C_{eq} = C_1 + C_2 = \frac{b_2 \epsilon_0 (b_1 + x(1 - \epsilon_r))}{h} \tag{3.3}$$

where $\epsilon_0 = 8.854 \cdot 10^{-12}$ F/m is the dielectric permictivity of the void and ϵ_0 is the dielectric permictivity of the material inside the capacitor.
With the mathematical relation to calculate the overall capacitance it is possible to define the time constant of the circuit as

$$\tau = RC_{eq} \tag{3.4}$$

When the time constant is known, the charge transient of the capacitor can be defined in the following form:

$$V_{out} = V_{dd} \left(1 - e^{-\frac{t}{\tau}}\right) \tag{3.5}$$

where V_{dd} is the supply voltage for the circuit. As can be seen in Equation 3.5, the output voltage of the capacitor increases with an exponential trend, starting from the zero value, up to V_{dd}.
In Figure 3.3 is represented the generic trend of a transient charge, given a specific time constant τ and choosing a supply voltage of 2.0 V.

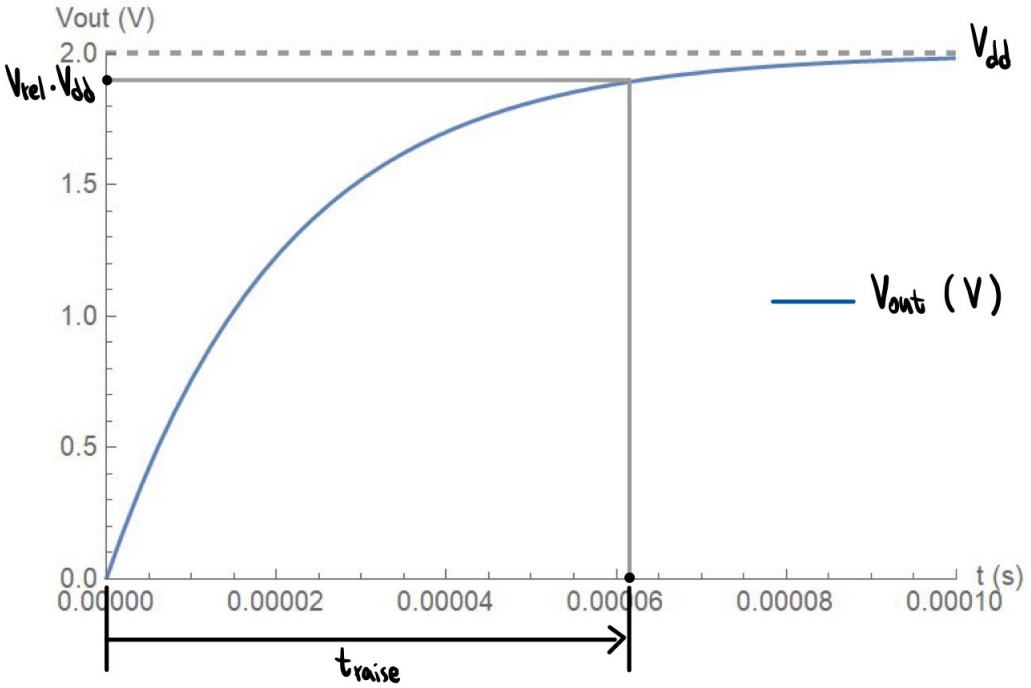

Figure 3.3: Charge transient

Although the time constant is a function of the displacement x, this graph helps to comprehend the overall idea behind this type of transducer, which is to stop the charge of the capacitor to a fraction value of the supply voltage, which is $V_{\mathrm{rel}} \cdot V_{\mathrm{dd}}$, and measure the time needed to reach this value, defined as $\mathrm{t_{raise}}$.
It is possible to define mathematically $\mathrm{t_{raise}}$ placing $\mathrm{V_{out}}$ of Equation 3.5 equal to $\mathrm{V_{rel}}$*$\mathrm{V_{dd}}$:

$$\mathrm{t_{raise}} = \tau \ln\left(\frac{1}{1-\mathrm{V_{rel}}}\right) \tag{3.6}$$

where $0 \leq \mathrm{V_{rel}} \leq 1$.
Remembering Equation 3.4, $\mathrm{t_{raise}}$ can be written as a function of the displacement x, defining the relation Input/Output of the transducer:

$$\mathrm{t_{raise}} = \frac{\mathrm{b1b2}R\epsilon 0 \ln\left(\frac{1}{1-\mathrm{Vrel}}\right)}{h} + Rx \ln\left(\frac{1}{1-\mathrm{Vrel}}\right)\left(\frac{\mathrm{b2}\epsilon 0\epsilon \mathrm{r}}{h} - \frac{\mathrm{b2}\epsilon 0}{h}\right) \tag{3.7}$$

As can be seen from Equation 3.7, the dependency between the output (time of charge) and the input (displacement) of the transducer is linear.

3.2.2 Optimization

After defining the I/O relation of the transducer it is necessary to size it and find the optimal values of the resistance R and dielectric permictivity ϵ_r that minimize the charging time t_{raise} and the dissipated power by the resistor. To perform the minimization it is necessary to define a cost function as the one in Figure 3.4.

Function that increases the difference between maximum and minimum raise time:

```
Cost1[b1_, b2_, h_, εr_, R_] := traise[b1, b2, h, εr, 1, R] - traise[b1, b2, h, εr, 0, R];
```

Function that forces to have at least a number $n\tau$ of time constant for the discharge

```
Cost2[b1_, b2_, h_, εr_, R_] := If[R Cap[b1, b2, h, εr, 1] < Ts / (nτ + ln[1/(1-Vrel)]), 0, R Cap[b1, b2, h, εr, 1]]
```

Function that lowers the power consumption

```
Cost3[R_] := 1 / R;
```

Overall target function

```
Target[b1_, b2_, h_, εr_, R_] := -W1 Cost1[b1, b2, h, εr, R] + W2 Cost2[b1, b2, h, εr, R] + W3 Cost3[R];
```

Figure 3.4: Cost functions

The overall cost function, defined as "Target" in Figure 3.4, takes into account three different functions:

1. Cost1 → to maximize the difference between maximum and minimum raise time → the system needs to have a fast response, so τ should be as low as possible
2. Cost2 → a number n of time constant (n_τ) is given in order to have a complete discharge of the capacitor
3. Cost3 → to minimize the power dissipation of the resistor

It should be noted that "Cost1" is to be maximized. Since a minimization is performed, the weight/penalty of this function is negative. Moreover, the minimum charging time is when x is minimum (x=0), while the maximum charging time is when x is maximum (x=b_1).
To perform the minimization the following constraints have been considered:

$$\begin{cases} 1mm \leq b_2 \leq 10mm \\ 0.1mm \leq h \leq 1mm \\ 1 \leq \epsilon_r \leq 10000 \\ 1\Omega \leq R \leq 10^7\Omega \end{cases}$$

Table 3.1 shows the results of the optimization process for different combinations of values of V_{rel}, f_s, n_τ, and fixing the maximum displacement b_1=2 mm and the supply voltage V_{dd}=1.8 V.

Parameter	Combination				
	1	**2**	**3**	**4**	**5**
V_{rel}	0.90	0.95	0.9	0.9	0.8
f_s(Hz)	4000	4000	4000	1000	2000
n_τ	8	8	10	8	9
b_2(mm)	3.0	10	10	1.0	10
h(mm)	0.70	1.0	1.0	1.0	1.0
ϵ_r	4500	10000	10000	10000	10000
R(Ω)	70000	12700	11400	53000	26000
$t_{raise,min}$(ns)	12.3	6.1	4.7	22.3	7.6
$t_{raise,max}$(ns)	55781.1	68111.2	46771.5	223496	75849.3
$f_{c,min}$(Hz)	$1.2 \cdot 10^9$	$9.6 \cdot 10^8$	$1.4 \cdot 10^9$	$2.9 \cdot 10^8$	$8.6 \cdot 10^8$

Table 3.1: Optimization results

$f_{c,min}$ is the minimum operating frequency of the binary counter, necessary to keep up with capacitor charging and subsequent sampling, defined as

$$f_{c,min} = \frac{2^{bits}}{t_{raise,max} - t_{raise,min}} \tag{3.8}$$

where "bits" indicates the resolution of the binary counter in terms of number of bits. It is possible to compute the number of bits of resolution with the following Equation:

$$\text{bits} = \frac{measurement \quad range}{instrument \quad resolution} \tag{3.9}$$

With a measurement instrument with a maximum resolution of 50 nm over a measurement range of 2 mm, the resolution of the binary counter should be 16 bits.
As can be seen from Table 3.1, the binary counter frequency is in the order of GHz, particularly it varies in the range $[0.29 - 1.4]$ GHz. Because the binary counter needs to count from 0 to 2^{16}-1 binary numbers, it is necessary to count at those frequencies at least, and that is the reason why f_c is that high. Through the implementation of modern processors it should not be a problem to develop a binary counter with an operating frequency of the order of GHz.

3.2.3 *Matlab* simulations

Figure 3.5 shows the *Simulink* model of the capacitor transducer.

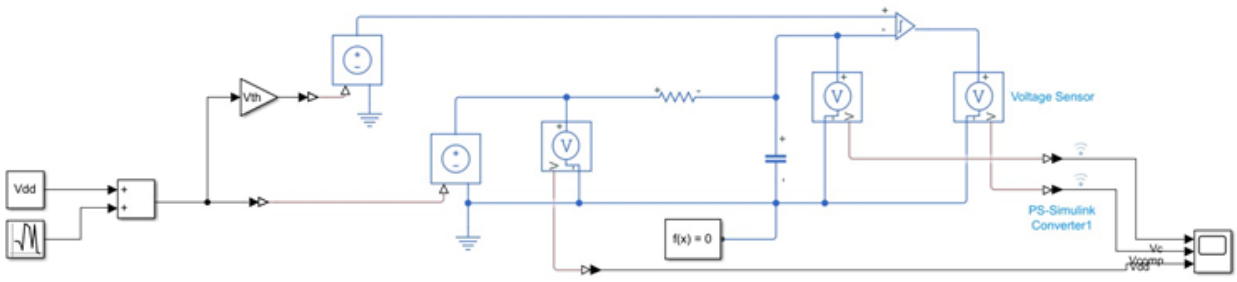

Figure 3.5: *Simulink* model of the capacitor transducer

As can be seen from Figure 3.5, the model considers a white noise effect, which is normally distributed and is added to the supply voltage V_{dd}. The stochastic contribution of the noise affects also the threshold voltage of the comparator, already defined in Subsection 3.2.1 as V_{ref}. Multiple simulations have been performed considering different values of V_{ref} in order to verify the linear dependency between the measured time and the displacement using a fitting linear model. The results of the simulations have then been compared to the expected theoretical values as can be seen in Figure 3.6.

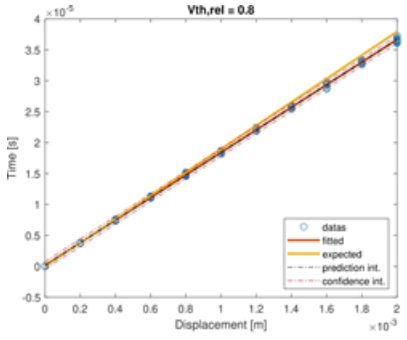

(a) Simulation with a threshold voltage of 0.8 V

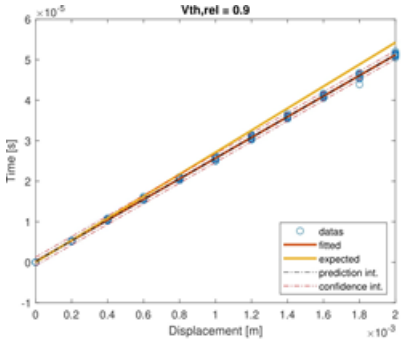

(b) Simulation with a threshold voltage of 0.9 V

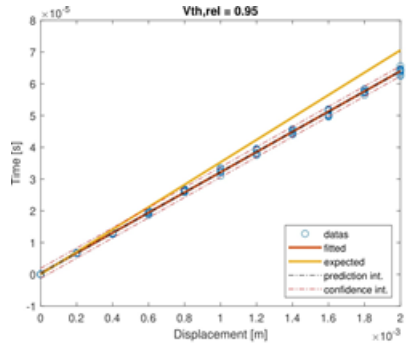

(c) Simulation with a threshold voltage of 0.95 V

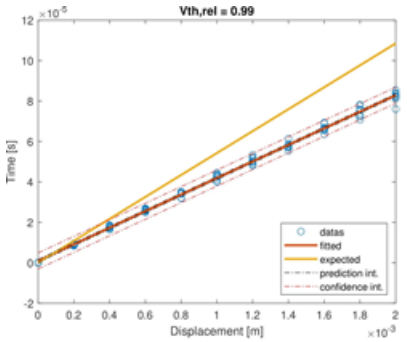

(d) Simulation with a threshold voltage of 0.99 V

Figure 3.6: *Matlab* simulations to verify the linear response of the transducer

As can be seen from Figure 3.6, decreasing the threshold voltage the uncertainty of the measures

improves, with the drawback of decreasing the time that has to be measured by the system. It can also be noted that, with the increasing of the threshold, the samples are more spread out and with a known constant uncertainty.

3.2.4 Uncertainty analysis

Starting from Equation 3.7, it is possible to reverse it and compute the displacement as a function of time:

$$x(t) = \frac{h \cdot t}{b_2 R \epsilon_0 \left(\epsilon_r - 1\right) \ln(\frac{1}{1-V_{rel}})} - \frac{b_1}{(\epsilon_r - 1)} \tag{3.10}$$

In this way it is possible to compute the uncertainty of the measure as the combination of the error related to time measures and the one related to the white noise which affect the threshold value.

$$\delta_x = \sqrt{\left(\frac{\partial x}{\partial t}\delta_t\right)^2 + \left(\frac{\partial x}{\partial V_{\text{rel}}}\delta_{V_{\text{rel}}}\right)^2} \tag{3.11}$$

where the first term is $\frac{\partial x}{\partial t}\delta_t$ and the second term is $\frac{\partial x}{\partial V_{\text{rel}}}\delta_{V_{\text{rel}}}$.
Deriving the displacement in time we get

$$\frac{\partial x}{\partial t} = \frac{h}{b_2 R \epsilon_0 \left(\epsilon_r - 1\right) \ln(\frac{1}{1-V_{rel}})} \tag{3.12}$$

which is constant, while the relative uncertainty of time (δ_t), assuming a uniform distribution of the error, it depends on the counting frequency of the circuit whose minimum value must withstand the characteristic of the transducer:

$$\delta_t = \frac{1}{f_c\sqrt{12}} \tag{3.13}$$

Deriving the displacement with respect to V_{rel} we get

$$\frac{\partial x}{\partial V_{\text{rel}}} = \frac{h \cdot t}{b_2 R \epsilon_0 \left(V_{rel} - 1\right) \left(\epsilon_r - 1\right) \ln^2(\frac{1}{1-V_{rel}})} \tag{3.14}$$

which increases with time, explaining the simulations results of Figure 3.6, while the relative uncertainty of the threshold voltage depends on the quality of the supply voltage in the following form:

$$\delta_{V_{\text{rel}}} = V_{rel} \cdot \delta_{V_{\text{dd}}} \tag{3.15}$$

It can be shown that the uncertainty $\delta_{V_{\text{rel}}}$ tends to be predominant respect to δ_t because it has higher values and is more difficult to control because it depends on the threshold standard deviation which cannot be assessed because it involves to know at a fundumental level the behavior of the circuit.
Figure 3.7 shows an example of the dependency of δ_x over time considering different values of $\delta_{V_{\text{rel}}}$ and a time uncertainty δ_t=120 ps, which means considering a counting frequency f_c=1.2 Ghz.

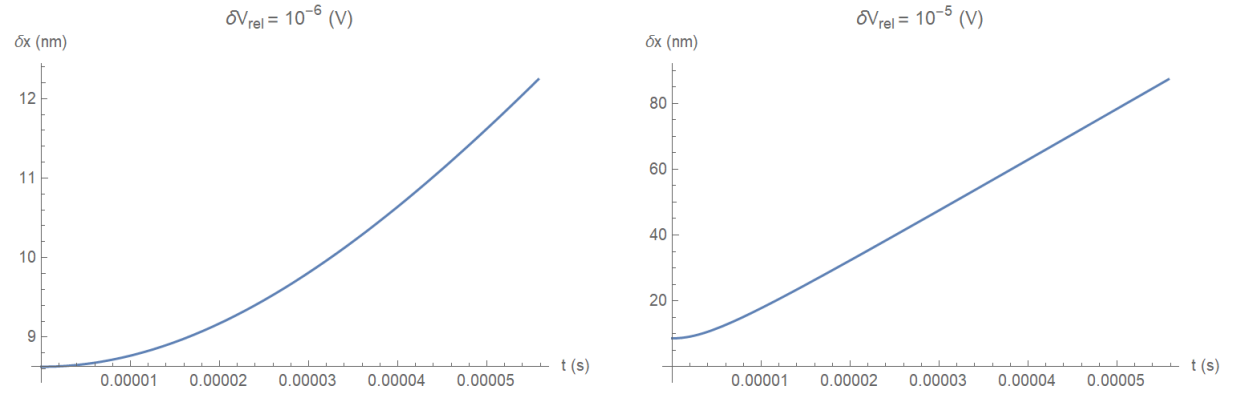

(a) Uncertainty of the displacement with $\delta_{V_{\text{rel}}} = 10^{-6}$ V **(b)** Uncertainty of the displacement with $\delta_{V_{\text{rel}}} = 10^{-5}$ V

Figure 3.7: Uncertainty of the displacement as a function of the measured time considering different values of $\delta_{V_{\text{rel}}}$

As can be seen from Figure 3.7, when $\delta_{V_{\text{rel}}}$ increases, its contribution over δ_x also increases, infact the curve becomes more linear, while with lower values of $\delta_{V_{\text{rel}}}$, the curve tends to assume a trend for which the contribution of $\delta_{V_{\text{rel}}}$ over δ_x is smaller. Due to the fact that in this situation it is not possible to know the standard deviation of the threshold voltage, we can compute $\delta_{V_{\text{rel}}}$ for particular values of uncertainty of the measurement system with related confidence level, depending on the counting frequency, as shown in Table 3.2.

Uncertainty δ_x	Confidence level (coverage factor)	f_c (GHz)	$\delta_{V_{\text{rel}}}$
25 nm	95% (1.96)	1.2	$\leq 1.08{\cdot}10^{-6}$
		2	$\leq 1.34{\cdot}10^{-6}$
	99% (2.576)	1.2	$\leq 5.14{\cdot}10^{-7}$
		2	$\leq 9.45{\cdot}10^{-7}$
	99.73% (3)	1.2	NaN
		2	$\leq 7.52{\cdot}10^{-7}$
		4	$\leq 9.12{\cdot}10^{-7}$
50 nm	95% (1.96)	1.2	$\leq 2.76{\cdot}10^{-6}$
		2	$\leq 2.87{\cdot}10^{-6}$
	99% (2.576)	1.2	$\leq 2.00{\cdot}10^{-6}$
		2	$\leq 2.15{\cdot}10^{-6}$
	99.73% (3)	1.2	$\leq 1.62{\cdot}10^{-6}$
		2	$\leq 1.82{\cdot}10^{-6}$
		4	$\leq 1.89{\cdot}10^{-6}$
80 nm	95% (1.96)	1.2	$\leq 4.59{\cdot}10^{-6}$
		2	$\leq 4.66{\cdot}10^{-6}$
	99% (2.576)	1.2	$\leq 3.43{\cdot}10^{-6}$
		2	$\leq 3.52{\cdot}10^{-6}$
	99.73% (3)	1.2	$\leq 2.90{\cdot}10^{-6}$
		2	$\leq 3.01{\cdot}10^{-6}$
		4	$\leq 3.05{\cdot}10^{-6}$

Table 3.2: $\delta_{V_{\text{rel}}}$ for different combinations of f_c, δ_x and confidence level

Chapter 4

Conclusions

To conclude this report, which is mainly based on the presentation of the transducer on which the displacement measurement system is based, Figure 4.1a shows the CAD model of the double compound rectilinear spring obtained with the help of *Autodesk Inventor* after the computation of its parameters values through a minimization, performed in *Wolfram Mathematica* environment, considering two different materials: aluminium and steel. The double compound was then evaluated according to a static verification on displacement and yielding using the software *nTopology*, resulting in Figure 4.1b.

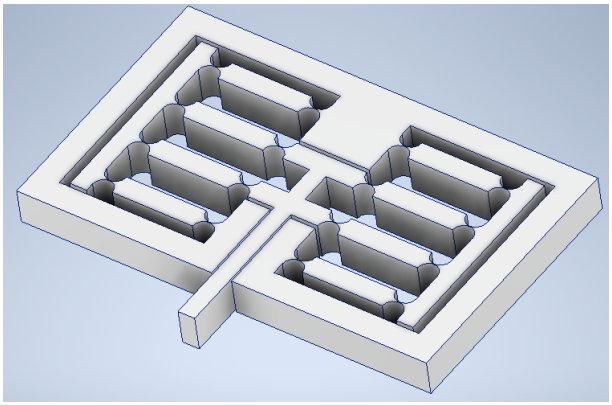

(a) CAD model

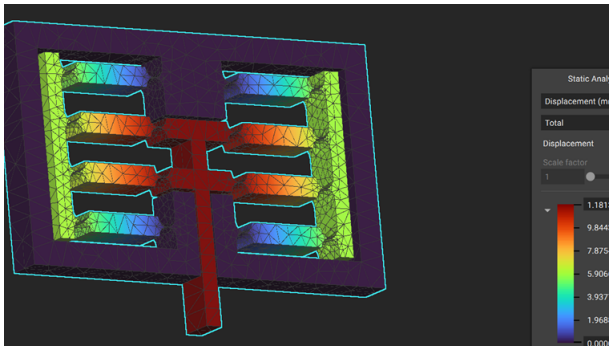

(b) Static verification

Figure 4.1: Double compound rectilinear spring

In conclusion, as a group it has been decided to focus the design of the linear displacement measurement system on the design of the transducer, whose aim is to convert the displacement into a measurable signal through time, and on the double compound rectilinear spring in order to provide the linear motion of the probe tip. A schematic of the electronic components, shown in Figure 3.1, was also provided in order to describe how the transducer works and how signal sampling is implemented through the use of a binary counter. As can be seen from Table 3.1, the transducer works typically with charging times which goes from 4.7ns to 223.5μs, therefore needing a binary counter with an operating frequency in the order of 10^1GHz, in order to keep up with the charging of the capacitor and not loose counts. Nowadays it should not be a problem to find a binary counter with such an operating frequency.